HHS Public Access

Author manuscript

Neurobiol Dis. Author manuscript; available in PMC 2023 June 26.

Published in final edited form as:

Neurobiol Dis. 2023 April ; 179: 106057. doi:10.1016/j.nbd.2023.106057.

CCR5 deficiency normalizes TIMP levels, working memory, and gamma oscillation power in APOE4 targeted replacement mice

Griffin A. Greco[a], **Mitchell Rock**[b,1], **Matthew Amontree**[b,c,1], **Maria Fe Lanfranco**[d], **Holly Korthas**[c], **Sung Hyeok Hong**[e], **R. Scott Turner**[f], **G. William Rebeck**[c,d], **Katherine Conant**[c,d,*]

[a]Georgetown University School of Medicine (GUMC), Department of Pharmacology, United States of America

[b]GUMC, United States of America

[c]Interdisciplinary Program in Neuroscience, United States of America

[d]GUMC, Department of Neuroscience, United States of America

[e]GUMC, Department of Biochemistry and Molecular & Cellular Biology, United States of America

[f]GUMC, Department of Neurology, United States of America

Abstract

The *APOE4* allele increases the risk for Alzheimer's disease (AD) in a dose-dependent manner and is also associated with cognitive decline in non-demented elderly controls. In mice with targeted gene replacement (TR) of murine *APOE* with human *APOE3* or *APOE4*, the latter show reduced neuronal dendritic complexity and impaired learning. *APOE4* TR mice also show reduced gamma oscillation power, a neuronal population activity which is important to learning and memory. Published work has shown that brain extracellular matrix (ECM) can reduce neuroplasticity as well as gamma power, while attenuation of ECM can instead enhance this endpoint. In the present study we examine human cerebrospinal fluid (CSF) samples from *APOE3* and *APOE4* individuals and brain lysates from *APOE3* and *APOE4* TR mice for levels of ECM effectors that can increase matrix deposition and restrict neuroplasticity. We find that CCL5, a molecule linked to ECM deposition in liver and kidney, is increased in CSF samples from *APOE4* individuals. Levels of tissue inhibitor of metalloproteinases (TIMPs), which inhibit the activity of ECM-degrading enzymes, are also increased in *APOE4* CSF as well as astrocyte supernatants brain lysates from *APOE4* TR mice. Importantly, as compared to *APOE4*/wild-type heterozygotes,

[*]Corresponding author at: Interdisciplinary Program in Neuroscience, United States of America, kec84@georgetown.edu (K. Conant).
[1]Equal contribution.

Declaration of Competing Interest

There are no competing financial interests for any of the authors in relation to the work described.

CRediT authorship contribution statement

Griffin A. Greco: Conceptualization, Validation, Formal analysis, Investigation, Data curation, Writing – original draft, Writing – review & editing. **Mitchell Rock:** Validation, Formal analysis, Investigation, Data curation, Writing – review & editing. **Matthew Amontree:** Validation, Formal analysis, Investigation, Data curation, Writing – review & editing. **Maria Fe Lanfranco:** Resources, Writing – review & editing. **Holly Korthas:** Software, Formal analysis. **Sung Hyeok Hong:** Investigation. **R. Scott Turner:** Resources. **G. William Rebeck:** Writing – review & editing, Resources, Supervision, Funding acquisition. **Katherine Conant:** Conceptualization, Writing – original draft, Writing – review & editing, Supervision, Funding acquisition.

APOE4/CCR5 knockout heterozygotes show reduced TIMP levels and enhanced EEG gamma power. The latter also show improved learning and memory, suggesting that the CCR5/CCL5 axis could represent a therapeutic target for *APOE4* individuals.

Keywords

Extracellular matrix; CCR5; APOE; MMP; TIMP-1

1. Introduction

Alzheimer's disease (AD) is a leading cause of dementia and by 2050, it will affect approximately 50% of individuals by age 85 (Brookmeyer et al., 2007). While the most significant risk factor for AD is age, the greatest genetic risk factor for AD is a genetic variant of apolipoprotein E (*APOE*), which encodes a protein responsible for lipid transport (Corder et al., 1993; Poirier et al., 1993; Rebeck et al., 1993; Strittmatter et al., 1993).

In contrast to mice, humans have three different isoforms of *APOE*: E2, E3, and E4. These differ by a single amino acid substitution at the 112th and 158th positions. The *APOE4* allele enhances the risk for developing AD (Rebeck et al., 1993; Strittmatter et al., 1993) while the *APOE2* allele diminishes this risk (Poirier et al., 1993). Interestingly, *APOE* variants also influence the age of onset of AD, so that *APOE4* carriers tend to get AD at earlier ages as compared to non-*APOE4* carriers (Poirier et al., 1993). Consistent with this observation, *APOE* genotype is thought to affect early processes in AD pathogenesis, such as Aβ accumulation or clearance (Kim et al., 2009).

APOE may also affect brain structure and function independent of amyloid deposition. *APOE4* has been associated with increased cognitive decline in elderly *APOE4* carriers who do not have AD (Plassman et al., 1997). Carriers in their 50s–60s, who are cognitively normal, show reduced glucose metabolism in parietal, temporal and prefrontal cortices (Small et al., 1995; Caselli et al., 2001). *APOE* genotype also alters the volume of the entorhinal cortex prior to the development of AD (Shaw et al., 2007). In murine studies, *APOE4* TR mice show neuronal simplification in the amygdala (Wang et al., 2005), and cortex (Dumanis et al., 2009). Furthermore, *APOE4* TR mice have abnormalities in hippocampal long-term potentiation (LTP) (Trommer et al., 2004; Trommer et al., 2005; Korwek et al., 2009). Importantly, *APOE4* TR mice have reduced sharp-wave ripple (SWR) abundance and low gamma power, brain rhythms important to memory consolidation and working memory (Gillespie et al., 2016; Jones et al., 2019). Intriguingly, reduced SWR abundance in these animals occurred at a relatively young age and the magnitude of reduction correlated with the magnitude of later cognitive impairment (Jones et al., 2019). In addition, gamma power may be reduced in AD and animal models the same (Klein et al., 2016; Murty et al., 2021; Traikapi and Konstantinou, 2021).

Accumulating evidence suggests that *APOE4* may be associated with low grade inflammation and glial activation (Tai et al., 2015). Of interest, both activated astrocytes and microglia secrete CCL5 (Lanfranco et al., 2017), a chemotactic cytokine that potently restricts neuroplasticity and LTP (Zhou et al., 2016; Shen et al., 2022). CCL5 also inhibits

pyramidal cell excitability which could in turn modulate gamma power and SWR abundance (Zhou et al., 2016). CCL5 has also been linked to excess ECM deposition (Passman et al., 2021; Bonnard et al., 2022). Neuronal extracellular matrix (ECM) exists in diffuse and condensed forms and both types can restrict neuroplasticity (Miyata and Kitagawa, 2017). For example, dendritic arbor is increased in mice with reductions in ECM-dense perineuronal nets (PNNs) (Alaiyed et al., 2020), which are predominantly localized to parvalbumin (PV) expressing inhibitory interneurons and increase their excitability through varied mechanisms (Bozzelli et al., 2018). Importantly, enzymatic digestion of brain ECM increases the power of *in vivo* cortical gamma oscillations (Lensjo et al., 2017) and the abundance of *ex vivo* hippocampal SWRs (Sun et al., 2018).

ECM levels are modulated by deposition as well as degradation, and the latter is mediated by metalloproteinases including matrix metalloproteases (MMPs) and A Disintegrin And Metalloproteases (ADAMs) (Rivera, 2019). These enzymes are zinc-dependent secreted or transmembrane endoproteases that have been well-studied for their ability to process ECM proteins but are now appreciated to act on a variety of soluble molecules and cell surface receptors as well (Conant et al., 2015). Family members that have been particularly well-implicated in neuroplasticity include MMP-2, MMP-3 and MMP-9 (Nagy et al., 2006; Okulski et al., 2007; Conant et al., 2010; Smith et al., 2014; Wojtowicz and Mozrzymas, 2014; Murase et al., 2017; Wiera et al., 2017). MMP and ADAM activity is in turn inhibited by respective classes of tissue inhibitors of metalloproteinases (TIMPs). Previous research has demonstrated that CCL5 plays a role in increasing ECM deposition in liver and kidney (Passman et al., 2021; Bonnard et al., 2022), and its endogenous receptor CCR5 is also linked to reduced plasticity in the brain (Zhou et al., 2016). Thus it was of interest in this study to examine CCL5 levels as well.

In terms of specific MMPs, MMP-9 is of particular interest in that it is neuronal-derived and its expression and release and/or subsequent activation is increased with pyramidal neuron activity (Szklarczyk et al., 2002). It is released from pre- and post-synaptic stores and thus it likely targets synaptically localized adhesion molecules and glutamate inputs to PNN-enveloped PV cells. MMP-9 activity has been well-implicated in hippocampal dependent learning and memory as well as striatal- and amygdala-based learning (Nagy et al., 2006; Ganguly et al., 2013; Smith et al., 2014). While MMP-9 levels may be elevated with late-stage AD and correlated with inflammation (Weekman and Wilcock, 2016), late-stage increases are likely due to microglial activation and other events that instead lead to maladaptive enzyme localization at regions including the blood brain barrier.

In terms of the mechanisms by which MMPs can influence learning and memory, ECM- and PNN-independent effects have also been well-described. For example, MMPs can activate pro-neurotrophins (Lee et al., 2001). These enzymes can also cleave cell adhesion molecules to generate N-terminal fragments which serve as integrin-binding ligands (Lonskaya et al., 2013). Of interest, integrin signaling may be critical to MMP- induced LTP and dendritic spine expansion (Wang et al., 2008). MMP-1 dependent activation protease activated receptor-1 (PAR-1) can also increase dendritic arborization (Allen et al., 2016) as well as some forms of LTP (Almonte et al., 2013).

In the present study, our overall aim was to explore the possibility that CCL5 and other potential ECM effectors that limit pyramidal arbor, gamma power and SWR abundance may be elevated in *APOE4* humans and TR mice. We also investigated the possibility that reductions in CCR5, which is linked to excess ECM deposition in other end organs as well as reduced plasticity in the brain (Passman et al., 2021; Bonnard et al., 2022; Shen et al., 2022), might rescue biochemical, neurophysiological and/or behavioral alterations associated with this allele.

2. Materials and methods

2.1. Human CSF samples

Human CSF samples were collected for a randomized placebo-controlled double-blind, multi-site, phase 2 trial of resveratrol in individuals with mild to moderate dementia due to AD (Turner et al., 2015). Resveratrol is a naturally occurring compound that is thought to work through a variety of mechanisms, including activation of sirtuins, which are proteins that regulate gene expression and may play a role in aging and age-related diseases. We did not utilize any samples from individuals treated with resveratrol; this clinical trial was just essential in providing a significant number of CSF samples from individuals with a known APOE genotype and demographic information. Concomitant use of FDA-approved medications for AD (*e.g.*, cholinesterase inhibitors) was allowed. The two randomized groups were similar at baseline with the exception that duration of diagnosis was longer in the placebo group. Participants (total $N = 119$) were randomized to placebo or resveratrol 500 mg orally once daily (with a dose escalation by 500-mg increments every 13 weeks, ending with 1000 mg twice daily). The total treatment duration was 52 weeks. For data presented herein we analyzed the pretreatment samples (Figs. 1 a–c, 2a and 2c), or alternatively after pretreatment stocks were depleted, the 52-week post placebo-treated individuals (Fig. 2b and d–g).

2.2. Mice

Strains used for this study included C57BL/6 J mice expressing human *APOE2*, *APOE3* or *APOE4,* under the control of the endogenous murine *APOE* promoter, that have been previously validated (Xu et al., 1996; Sullivan et al., 1997). Murine APOE, which is functionally different than human isoforms (Tcw et al., 2022), has been replaced in these mice so that different TR mice are typically compared to each other as opposed to wild type murine APOE expressing animals (Dumanis et al., 2009). We also used strains from the Jackson Laboratory. Mice obtained from Jackson Laboratories included wild-type/C57BL6J background or *CCR5* knockout (KO) mice on a C57BL6J background. *APOE4* TR mice were also crossed with wild-type or *CCR5* KO mice to generate mice either with (1) a heterozygous TR of *APOE4* on a wild-type background or (2) a heterozygous TR of *APOE4* and a heterozygous KO of *CCR5*. Mice were housed four-five per cage. Food and water were provided *ad libitum*. Experimental groups were matched in terms of age and male to female ratio for each comparison and arbitrarily assigned to groups. Studies were performed on mice of approximately 6 months of age, with the male to female ratio balanced in all studies except EEG experiments. Due to considerations of sample size and the issue of implant/mouse size, we used all male mice for EEG studies. Experiments were performed

in accordance with National Institutes of Health guidelines and institutionally approved protocols (2016–1117 and 2018–0037). Cages were supplied with balconies and nesting materials for enrichment. Mice were anaesthetized with isoflurane and insensitivity to deep pain was confirmed prior to euthanasia by rapid decapitation.

2.3. Primary astrocyte cultures

Primary astrocytes from 1 to 2 day old *APOE* TR mice were prepared as previously described (Lanfranco et al., 2021) and then stored in liquid nitrogen. For studies herein, 2 vials for each genotype were rapidly thawed and added to pre-warmed (37 °C) medium (Gibco Minimal Essential Medium with 10% fetal calf serum and 1× penicillin streptomycin). Astrocytes were plated onto 6 well Costar plates. At confluence, the media was changed and supernatant samples were taken 12 h subsequently for ELISAs.

2.4. Brain lysates

Following euthanasia, hippocampi and cortices were micro-dissected. Regional lysates were prepared by lysis in immunoprecipitate buffer [50 mM Tris, pH 7.5, 150 mM NaCl, 0.1% sodium dodecyl sulfate, 1% octylphenoxypoly (ethyleneoxy) ethanol, branched, and 1× protease and phosphatase cocktail (Thermo Scientific 1,861,281)]. Lysates were sonicated for 10 s, placed on ice for 20 min, and centrifuged 15 min at 14,000 rpm at 4 °C. Lysate supernatants were saved for protein analyses.

2.5. ELISA and Western blot

Specific protein concentrations in CSF samples and tissue lysates were measured by ELISA (R & D Systems, Minneapolis MN), performed according to the manufacturer's instructions with the following changes. The incubation of sample with the antibody coated well was in the 4 °C cold room overnight. In addition, the volume of sample added was 30 μl for murine lysates with 70 μl assay buffer. Note, that for each ELISA, all samples were run on a single plate to limit inter-experimental variability. Catalog numbers were as follows: murine TIMP-1, MTM100; murine MMP-9, MMP900B; murine CCL5, MMR00; human TIMP-1, DTM100; human TIMP-3, DY973, human MMP-9, DY11–05; human CCL5, DRN00B. For immunoblotting, 20 μl CSF was mixed with Laemmli sample buffer (Bio-Rad, Hercules, CA, USA, catalog #161–0737) containing 5% β-mercaptoethanol, and boiled for 5 min at 95 °C. Samples were subsequently separated by electrophoresis on precast gels (4–20% mini protein TGX gels, Bio-Rad catalog #456–1094) and transferred to nitrocellulose membranes (Trans-Blot Turbo Transfer, Bio-Rad, catalog #1704159). Membranes were probed with primary and secondary antibodies, and bands visualized by chemiluminescence as previously described (Alaiyed et al., 2019). We utilized a primary antibody to human brevican (1:1000, ThermoFischer PA5–4753). For densitometric normalization, since more than one gel was required to compare *APOE3/E3 versus APOE4/E4* CSF samples by Western blot, we divided each band at the same molecular weight by the average of all *APOE3/E3* band densities at that molecular weight for each individual image.

2.6. Zymography

Gelatin (denatured collagen IV) substrate zymography was performed using precast gels from Invitrogen/Novux. 10% gels with 50 μl wells were loaded with 45 μl sample prepared from a mixture of 25 μl CSF and 25 μl zymogram sample buffer (BioRad). Samples were separated by electrophoresis and gels were then extracted and incubated for 30 min in renaturation buffer (Novux) followed by 3 days in development buffer (Novux) at 37 °C. The relatively long development was necessary for the visualization of MMP-9 activity.

2.7. T-Maze

Working memory was assessed in these mice using the T maze (Shoji et al., 2012). The task was performed by placing a mouse at the base of the T apparatus, and allowing the mouse to traverse down the length of the maze and explore either the left or right side of the T. Immediately following the mouse's choice of goal arm, a door placed above each side of the maze was closed and the mouse was allowed to explore the side for 30s. The mouse was then removed before sanitizing the entire apparatus, after which the mouse was placed at the beginning of the T again to repeat the task. This version of the task does not involve utilizing a reward, and for each subsequent trial following the first, data is recorded as either a 1 or 0 to indicate whether the mouse spontaneously alternated arms of the maze or not. This task was repeated in random order for alternating cohorts of mice, and the data are presented as an average percent of alternation over the course of 4 trials.

2.8. Fear conditioning

Long-term hippocampal-dependent memory was assessed using fear conditioning (FC). Briefly, the training day for FC began with mice placed in the FC apparatus and allowed to explore the novel environment containing patterned walls for 180 s. Following the acclimatization period, mice received a mild shock (0.5 mA, 1 s) at 180 s, 240 s, and 300 s, before being removed from the apparatus after 360 s. For the entirety of the training period, mice were video recorded and monitored using ANY-maze software, which measured bouts of freezing (defined as the mouse being immobile for >1 s), the total duration of freezing, and latency to freeze. Long-term memory was assessed three days later when mice were placed in the same FC chamber with the contextual environment, and the same metrics were measured over a 180 s period in the absence of floor shocks.

2.9. In vivo EEG recordings

Telemetry recordings were performed with a DSI telemetry system connected to LabChart (AD Instruments) acquisition software *via* a Physiotel Bridge. We utilized mouse-sized implant transmitters which allowed for EEG and EMG recordings. The transmitter was placed subcutaneously in the lower back region and the electrodes were tunneled back towards the head. Surgery was performed by a D.V.M./Ph.D. veterinary surgeon (S.H. Hong) with sterile technique and general anesthesia continuous inhaled isoflurane), pre- and post-operative pain relief, and prophylactic antibiotics. Sutures were used to close the surgical wound and removed 10–14 days after surgery. A differential EEG configuration was recorded (L Frontal to R Parietal) from epidural screws, and EMG electrodes were placed in the cervical trapezius muscle. Video records were captured simultaneous with

EEG. Signal was detected from implants (wirelessly) through a pad beneath the standard mouse housing units. Mice were able to see each other through clear housing units and are provided with enrichment. Signals were recorded and stored in LabChart format for offline data analysis. Data analysis included appropriate filtering and calculation of power in specific frequency ranges. After full recovery from surgery (3 days) low gamma power (20–55 Hz) was calculated for a 60-min interval once every two hours during the dark/active phase (6 pm- 6 am and the average of power from $n = 6$ one-hour recording epochs recorded for each day.

2.10. Statistics

Sample size was based on power analyses for expected differences in human CSF and murine lysate values based on our prior published studies of inflammatory molecules for mu and sigma values (Conant et al., 1999; Alaiyed et al., 2020). For CSF analyses, the alpha value was 0.05 and desired power set at 0.80 as suggested at https://www.stat.ubc.ca/~rollin/stats/ssize/n2.html. All data were entered into a GraphPad Prism 9.0 program and statistical analysis was performed using Student's unpaired *t*-test for two group comparisons or ANOVA, with post-hoc analyses as indicated, for comparisons of more than two groups. Significance was set at $p < 0.05$ and ROUT testing was performed to identify outliers (Q = 0.1% for CSF; Q = 1% for other analyses). For correlation analyses, Pearson correlation analyses were performed.

3. Results

3.1. APOE4 is associated with elevated CSF levels of CCL5 and TIMP-1

To evaluate the possibility that CCL5 or other potential ECM effectors that may limit plasticity are elevated in association with *APOE4*, we first performed ELISA analysis of human CSF samples obtained from *APOE*-genotyped individuals with mild to moderate AD. Patient demographics are outlined in Table 1. As shown in Fig. 1, *APOE4/E4* AD patients have significantly higher CCL5 protein concentrations detected in CSF as compared to *APOE3/E3* and *APOE3/E4* AD patients ($p < 0.0001$ and $p = 0.0012$, respectively), as measured by ELISA. *APOE4/E4* AD patients also have elevated levels of TIMP-3 protein concentrations as compared to *APOE3/E3* and *APOE3/E4* AD patients ($p < 0.0001$ and $p = 0.0068$, respectively), as detected by ELISA. Furthermore, both *APOE3/E4* and *APOE4/E4* AD patients have significantly higher TIMP-1 protein concentration, as compared to *APOE3/E3* patients ($p = 0.0049$ and $p = 0.0033$, respectively). Though it did not reach statistical significance, the *p* value for the Pearson correlation of CCL5 with TIMP-1 was 0.1436 ($n = 77$, $r = 0.1682$, R^2 = 0.0283) and for CCL5 with TIMP-3 it was 0.1257 (n = 77, $r = 0.176$, R^2 = 0.031). The lack of a correlation that reached statistical significance could be in part due to sample size or to common genetic polymorphisms that have a large effect on basal TIMP expression (Peterson et al., 2009; Lorente et al., 2013).

3.2. Specific matrix degrading molecules are not concomitantly increased in CSF samples from APOE4 positive individuals

Depending on the stimulus or disease, the expression and activity of matrix degrading molecules can change with TIMPs in a concordant or discordant fashion. To evaluate the

possibility that MMPs might be concomitantly increased to abrogate effects of elevated TIMPs, we examined MMP levels in CSF samples from *APOE*-genotyped individuals. There was no difference in MMP-1, MMP-2 or MMP-9 protein levels as a function of AD *APOE* patient genotype in our sample group (Figs. 2a–c, ANOVA with Tukey's multiple comparisons test). Note fewer samples were analyzed for MMP-2 because many pre-treatment samples had been depleted and thus 52-week post-placebo samples were instead used for this assay as described in the methods section. The post-placebo patient demographics are shown in Table 2. We also performed gelatin-based zymography for *APOE4/E4* and *APOE3/E3* individuals (Fig. 2d). This assay allowed for quantitation of pro and active forms of MMP-2 and MMP-9. While we did not detect a significant difference in either, active MMP-9 levels appeared slightly diminished in *APOE4/E4* individuals (Fig. 2e, $p = 0.07$). Because gelatin-zymography is limited by a denaturation step that imparts activity to pro-forms and may also dissociate TIMPs from MMPs, we also looked at MMP-9 substrate cleavage as a function of *APOE* genotype. Results for brevican, which is cleaved by MMP-9 and other metalloproteases (Nakamura et al., 2000), are shown in Figs. 2f and g. In brain extracts, particulate brevican may be membrane-linked and/or contribute to insoluble lattices including PNNs (Seidenbecher et al., 1995), while soluble brevican, the majority form, may also access the CSF compartment. Both forms may be cleaved, and previous work has demonstrated reduced brevican cleavage in an animal model of AD (Ajmo et al., 2010). As shown in Fig. 2f, our blots show high molecular weight soluble brevican as well as a previously described approximately 50–60 kDa metalloprotease generated cleavage fragment (Seidenbecher et al., 1995; Ajmo et al., 2010; Hussler et al., 2022). The Ponceau is a representative image of overall protein transfer at approximately 50 kDa in the Western blot for brevican. This proteolytic fragment is significantly increased in *APOE3/3* as compared to *APOE4/E4* CSF samples ($p = 0.0039$, Student's *t*-test).

3.3. CCL5 and TIMP-1 are increased in astrocyte supernatants and brain lysates from APOE4 TR mice

To examine potential cellular sources of increased CCL5 and TIMP-1 expression as a function of *APOE* genotype, we also evaluated basal release of these molecules in astrocytes cultured from *APOE* TR mice. We focused on astrocytes since this cell type is numerous in the CNS and astrocytes can express both CCL5 and TIMP-1 (Crocker et al., 2006; Welser-Alves et al., 2011; Lanfranco et al., 2017; Hasel et al., 2021). As shown by ELISA analyses of culture supernatants (Fig. 3 a and b), astrocytes cultured from *APOE4/E4* TR mice release significantly more CCL5 and TIMP-1 as compared to those from *APOE3/3* TR mice (Fig. 3a and b). The difference between CCL5 levels in *APOE3/E3* and *APOE4/E4* astrocytes is significant at $p = 0.0095$ and the difference between *APOE2/E2* and *APOE4/E4* is significant at $p < 0.0001$ (ANOVA with Tukey's multiple comparisons *post hoc*). For TIMP-1, in which we only examined *APOE3/E3* and *APOE4/E4* supernatants, the difference is significant at $p < 0.0001$ (Student's t-test). Since astrocytes cultured from 1 to 2 day old pups likely differ from those in intact aged brain, we also examined hippocampal lysates from *APOE3/E3* and *APOE4/E4* TR mice. Results are shown in Figs. 3c–d and demonstrate that both CCL5 and TIMP-1 are increased in *APOE4/E4* TR lysates ($n = 14$, $p = 0.0029$ and 0.0069 respectively, Students t-test).

3.4. Gamma power is increased in CCR5 knockout mice

To evaluate the possibility that elevated CCL5 might influence gamma power in a manner observed in association with *APOE4* (Jones et al., 2019), we looked at gamma power in mice harboring a knockout of *CCR5*, the principal receptor for CCL5 in the brain. Our rationale for the use of this mouse model was based on increased CCL5 expression with *APOE4* as well as prior work demonstrating increased pyramidal excitability in this model (Shen et al., 2022). As shown in Fig. 4, gamma power (20–55 Hz) is significantly increased in *CCR5* knockout mice as compared to wild type ($p = 0.0063$; $n = 5$ per genotype). Note: EEG activity was recorded over a 2-week period, and gamma power was calculated for a 60-min interval once every two hours during the dark/active phase (6 pm- 6 am; average of power from $n = 6$ one-hour recording epochs) and averaged per day (4a). Days elapsed indicates EEG data recorded after animals had fully recovered from the implantation surgery and analgesia/anesthesia (3 days). The average value for each animal over all days is shown in 4b.

3.5. Gamma power (20 – 55 Hz) is significantly increased in APOE4/CCR5KO heterozygous mice as compared to age-matched APOE4/wild-type mice

To determine whether CCR5 knockout could increase gamma power in the background of *APOE4* expression, we compared EEG activity in *APOE4* TR/*CCR5*KO heterozygotes to that in *APOE4* TR heterozygotes on a wild type background. As shown in Fig. 5, gamma power (20 – 55 Hz) is significantly increased in *APOE4*/CCR5KO heterozygous mice as compared to age-matched *APOE4*/wild-type mice (5a; $p = 0.0062$; $n = 3$ per genotype). Gamma power was again calculated for a 60-min interval once every two hours during the dark/active phase (6 pm- 6 am; average of power from n = 6 one-hour recording epochs) and averaged per day. Days elapsed indicates EEG data recorded after animals had fully recovered from the implantation surgery. The average value for each animal over all days is shown in 5b.

3.6. APOE4/CCR5KO heterozygous mice show TIMP-1 normalization, as well as improved working memory and long-term memory in the T-maze and fear conditioning tasks

CCR5 is expressed on astrocytes (Lanfranco et al., 2017) and its engagement by endogenous ligands including CCL4 and CCL5 could contribute to their activation and expression of TIMP-1 (Crocker et al., 2006; Passos et al., 2009). We thus examined TIMP-1 levels in *APOE4* TR/*CCR5*KO heterozygotes and *APOE4* TR heterozygotes on a wild type background. As shown in Fig. 6, TIMP-1 levels are reduced in hippocampal lysates from *APOE4* TR/ CCR5 KO heterozygotes as compared to *APOE4* TR mice with normal CCR5 (6a). However, MMP-9 levels are not significantly different ($p = 0.5746$) between APOE4 TR/CCR5 KO heterozygotes (mean +/− SEM 165.3 +/− 35.21 pg/mg total protein) compared to APOE4 TR/wild-type mice expressing CCR5 (mean +/− SEM 140.3 +/− 25.96 pg/mg total protein), suggesting that the decreased TIMP-1 levels in the heterozygotes results in increased MMP-9 activity compared to mice with intact CCR5 signaling. In addition, working memory and long-term memory performance, in which we saw significant increases in alternation on the T maze and freezing episodes during the recall portion of fear conditioning (b-d), is consistent with improved memory in *APOE4* expressing mice

with reduced CCR5 expression. Moreover, Pearson correlation analyses of TIMP-1 and behavioral endpoints (6e–g) show a general trend between increased levels of TIMP-1 and worse cognitive performance which reaches significance for latency to freeze (alternation: R^2 = 0.1194, $p = 0.1744$; latency to freeze: R^2 = 0.2532, $p = 0.0395$; freezing episodes: R^2 = 0.1434, $p = 0.1340$).

4. Discussion

In the present study, we found that *APOE4* is associated with increased CCL5 and TIMP-1 levels in humans and TR mice, two molecules that have been shown to negatively regulate neuroplasticity (Okulski et al., 2007; Zhou et al., 2016). Consistent with this, decreasing the CCL5 receptor CCR5 increases MAPK/CREB signaling, LTP and the temporal window for memory linking (Zhou et al., 2016; Shen et al., 2022). Endogenous CCL5 also blocks neuronal calcium oscillations (Meucci et al., 1998). In addition, TIMP-1 has been shown to inhibit MMP-9 dependent LTP in prefrontal cortex (Okulski et al., 2007).

CCL5 and TIMP-1 might also increase ECM deposition to less directly restrict plasticity. Indeed, CCL5 is linked to increased ECM deposition in liver and kidney and TIMP-1 inhibits the activity of ADAMs and MMPs that cleave constituents of both dense and diffuse ECM (Knight et al., 2019; Passman et al., 2021; Bonnard et al., 2022). We also show here that *APOE4* is associated with increased levels of TIMP-3. Previous work has shown that TIMP-3, which inhibits ADAM –10 and ADAM-17, reduces α- secretase mediated cleavage of amyloid precursor protein (Hoe et al., 2007). TIMP-3 levels are also increased in cortical tissues from human AD brain (Hoe et al., 2007).

Importantly, we observed no commensurate increase in MMP-1, MMP-2 or MMP-9 in *APOE4* human CSF, suggesting that elevated levels of TIMP-1 and TIMP-3 likely reduce overall proteolysis by the MMPs with which they interact. This could have consequences not only on ECM regulation but, in the setting of potential amyloid formation, on amyloid levels. Similar to select ADAMs, MMP-9 acts as an α-secretase and is also one of the few proteases that can also degrade fibrillar amyloid (Yan et al., 2006; Yin et al., 2006). In related work, amyloid deposition is reduced in mice engineered to express high levels of MMP-9 (Fragkouli et al., 2014; Yang et al., 2015). Similarly in human CSF, MMP-2 which shares substrate similarity with MMP-9, is negatively correlated with amyloid deposition as assessed by Pittsburgh compound B labeling (Sasaki et al., 2021).

Depending on the population studied, previous studies also suggest that MMP-9 levels may be unchanged or reduced in AD patients as compared to controls (Adair et al., 2004; Mroczko et al., 2014). And though we acknowledge that other reports show that MMP-9 may be elevated at the blood brain barrier or in the brain parenchyma with human *APOE4*, AD or aggressive mouse models of the same (Halliday et al., 2016; Weekman and Wilcock, 2016; Montagne et al., 2020), potential confounds include elevated amyloid levels in aggressive murine models and/or select *APOE4* patient populations (Deb and Gottschall, 1996). In addition, the ability of MMP-9 to ameliorate or exacerbate disease pathology is likely a function of quantity as well as localization. For example, increased expression of MMP-9 by activated microglia or pericytes at the blood brain barrier could have detrimental

effects, while neuronal-derived and localized MMP activity may target preferentially target PNNs and synaptic adhesion molecules to enhance plasticity (Tian et al., 2007; Conant et al., 2015; Martin-de-Saavedra et al., 2022).

We also observed an effect of *APOE* genotype in primary astrocyte cultures (Fig. 3), suggesting that the regulation of ECM proteolysis could occur in part through astrocytic mechanisms. Astrocytes cultured from *APOE4/E4* TR mice had increased supernatant levels of CCL5 and TIMP-1, suggesting that this cell type could contribute to changes seen in human CSF and murine brain lysates. Of interest, all human *APOE* isoforms have been shown to attenuate inflammation (Yin et al., 2019) and given that *APOE4* levels are reduced in comparison to other isoforms (Riddell et al., 2008), glial activation may be more prominent in the background of this particular isoform.

The most promising findings, however, were the normalization of TIMP-1 levels, EEG gamma power, and working memory through partial knockdown of CCR5. *In vivo* and *ex vivo* gamma power is enhanced by ECM attenuation (Lensjo et al., 2017; Bozzelli et al., 2020) and is thought to be important to working memory and attention. Gamma entrainment through sensory stimulation also improves cognition in a murine model of AD (Iaccarino et al., 2016) and has more recently been shown to reduce PNN levels (Venturino et al., 2021). Moreover, gamma power is reduced in *APOE4/E4* knock-in mice and the magnitude of reduction correlates with subsequent cognitive impairment (Jones et al., 2019). Though we did not directly compare wild type and *APOE4/E4* TR mice in a single surgery day or experimental cohort, as compared to wild type mice, the *APOE4* TR/wild-type heterozygous animals had reduced gamma power (compare Figs. 5 and 6 in which wild type mice were generally over 0.005 mV^2 and *APOE4* TR/wild-type mice were generally below this threshold). While we did not investigate the effects of CCR5 reduction in *APOE3/E3* TR mice, and we acknowledge that AD relevant effects may not be limited to *APOE4*, we note that it may be especially important to normalize gamma power in *APOE4* individuals.

Though our study is mechanistic in terms of demonstrating that a reduction in CCR5 normalizes *APOE4* relevant endpoints, a limitation is that we do not identify the downstream molecular effectors of CCR5-dependent normalization. Increased TIMP levels in *APOE4/E4* TR mice with normalization by knockdown of CCR5, and prior publications linking TIMPs to ECM deposition and reduced plasticity, support a potential role for altered ECM regulation in *APOE4* TR mice as a contributor to behavioral and neurophysiological endpoints. This is supported by recently published work which shows chemokine and matrisome (ECM protein and associated factors) increases in human IPSC-derived *APOE4* astrocytes. This work also shows that *APOE4* microglia are enriched for ECM, chemokine and cytokine signaling pathways in multiple brain regions (Tcw et al., 2022). In addition, ECM changes including enrichment of select components and/or an association between chondroitin sulfate proteoglycans and plaques have been described in AD brain (DeWitt et al., 1993; Lepelletier et al., 2017; Hebisch et al., 2023). Additional mechanisms, however, may also be at play. For example, the effect of CCR5 antagonists on LTP are associated with an increase in MAPk/CREB activity in glutamatergic neurons that could influence our endpoints (Zhou et al., 2016). Indeed, work from the Silva group has shown that pyramidal cell excitability is increased in the setting of CCR5 reductions and increased MAPk/CREB

activity (Zhou et al., 2016). And as is the case for a reduction in inhibitory neuronal function, an increase in excitability of pyramidal neurons can enhance gamma oscillation power (Klemz et al., 2021). Hypothetical possibilities by which the CCL5/CCR5 axis may reduce neuronal excitability and gamma power are highlighted in the attached summary schematic (Fig. 7). It should also be noted, however, that while activation of the CCL5/CCR5 axis reduces plasticity in many studies, its activation may aid recovery following some forms of acute injury (Ho et al., 2021; Ping et al., 2021).

Future studies to address the downstream mechanisms by which CCR5 normalizes gamma power and cognitive endpoints in the *APOE4* TR mice should include interventions that specifically target the ECM (Dubisova et al., 2022) and examination of specific ECM proteins in fixed brain tissue from *APOE4* expressing humans. These experiments should also address PNN sulfation, which may be altered in AD and also influence endpoints including susceptibility to proteolysis (Foscarin et al., 2017; Logsdon et al., 2022; Scarlett et al., 2022).

In summary, we have demonstrated that CCL5 is increased in *APOE4* human CSF and brain lysates from *APOE4* TR mice and that biochemical, neurophysiological and behavioral deficits in heterozygous *APOE4* TR mice are normalized by heterozygous knockout of *CCR5*. We propose that it may be valid to consider use of the safe and well-tolerated CCR5 antagonist maraviroc, which promotes plasticity and/or is neuroprotective in mouse models of HIV and stroke (Joy et al., 2019; Bhargavan et al., 2021), in select *APOE4* positive individuals.

Acknowledgements

We would like to acknowledge outstanding veterinary support from the Department of Comparative Medicine and Dr. Patricia Foley. In addition, we would also like to apologize to investigators whose excellent work was not directly cited. We would also like to thank Tahiyana Khan and Dr. Patrick Forcelli for assistance in setting up the EEG recording software, Dr. Mark Burns for the use of his surgical area, and Christi Ann S Ng for shared resources. Katherine Conant, William Rebeck, and Griffin Greco received funds for support and/or supplies from NIH as follows: R01AG077002 (KC), R01 NS 100704 (GWR), and T32 NS 121780 (GAG).

CSF and plasma samples were collected with informed consent as a part of the Resveratrol clinical trial under Food and Drug Administration IND 104205, and registered at http://ClinicalTrials.gov (NCT01504854). All CSF samples were handled with strict anonymity throughout the study. APOE genotype and demographic data used in the preparation of this manuscript were obtained from the University of California, San Diego Alzheimer's Disease Cooperative Study (ADCS) Legacy database, supported by NIA U01AG010483 for the ADCS, ADCS funding sources, and funding by the ADCS. ADCS personnel including Dr. Robert Rissman contributed to the design and implementation of the ADCS and/or provided data but did not participate in analysis or writing of this report.

Data availability

Data will be made available on request.

References

Adair JC, Charlie J, Dencoff JE, Kaye JA, Quinn JF, Camicioli RM, Stetler-Stevenson WG, Rosenberg GA, 2004. Measurement of gelatinase B (MMP-9) in the cerebrospinal fluid of patients with vascular dementia and Alzheimer disease. Stroke 35, e159–e162. [PubMed: 15105518]

Ajmo JM, Bailey LA, Howell MD, Cortez LK, Pennypacker KR, Mehta HN, Morgan D, Gordon MN, Gottschall PE, 2010. Abnormal post-translational and extracellular processing of brevican in plaque-bearing mice over-expressing APPsw. J. Neurochem. 113, 784–795. [PubMed: 20180882]

Alaiyed S, McCann M, Mahajan G, Rajkowska G, Stockmeier CA, Kellar KJ, Wu JY, Conant K, 2020. Venlafaxine stimulates an MMP-9-dependent increase in excitatory/inhibitory balance in a stress model of depression. J. Neurosci. 40, 4418–4431. [PubMed: 32269106]

Allen M, Ghosh S, Ahern GP, Villapol S, Maguire-Zeiss KA, Conant K, 2016. Protease induced plasticity: matrix metalloproteinase-1 promotes neurostructural changes through activation of protease activated receptor 1. Sci. Rep. 6, 35497. [PubMed: 27762280]

Almonte AG, Qadri LH, Sultan FA, Watson JA, Mount DJ, Rumbaugh G, Sweatt JD, 2013. Protease-activated receptor-1 modulates hippocampal memory formation and synaptic plasticity. J. Neurochem. 124, 109–122. [PubMed: 23113835]

Bhargavan B, Woollard SM, McMillan JE, Kanmogne GD, 2021. CCR5 antagonist reduces HIV-induced amyloidogenesis, tau pathology, neurodegeneration, and blood-brain barrier alterations in HIV-infected hu-PBL-NSG mice. Mol. Neurodegener. 16, 78. [PubMed: 34809709]

Bonnard B, Ibarrola J, Lima-Posada I, Fernandez-Celis A, Durand M, Genty M, Lopez-Andres N, Jaisser F, 2022. Neutrophil gelatinase-associated Lipocalin from macrophages plays a critical role in renal fibrosis via the CCL5 (chemokine ligand 5)-Th2 cells-IL4 (interleukin 4) pathway. Hypertension 79, 352–364. [PubMed: 34794340]

Bozzelli PL, Alaiyed S, Kim E, Villapol S, Conant K, 2018. Proteolytic remodeling of Perineuronal nets: effects on synaptic plasticity and neuronal population dynamics. Neural Plast 2018, 5735789. [PubMed: 29531525]

Bozzelli PL, Caccavano A, Avdoshina V, Mocchetti I, Wu JY, Conant K, 2020. Increased matrix metalloproteinase levels and perineuronal net proteolysis in the HIV-infected brain; relevance to altered neuronal population dynamics. Exp. Neurol. 323, 113077. [PubMed: 31678140]

Brookmeyer R, Johnson E, Ziegler-Graham K, Arrighi HM, 2007. Forecasting the global burden of Alzheimer's disease. Alzheimers Dement. 3, 186–191. [PubMed: 19595937]

Caselli RJ, Osborne D, Reiman EM, Hentz JG, Barbieri CJ, Saunders AM, Hardy J, Graff-Radford NR, Hall GR, Alexander GE, 2001. Preclinical cognitive decline in late middle-aged asymptomatic apolipoprotein E-e4/4 homozygotes: a replication study. J. Neurol. Sci. 189, 93–98. [PubMed: 11535238]

Conant K, McArthur JC, Griffin DE, Sjulson L, Wahl LM, Irani DN, 1999. Cerebrospinal fluid levels of MMP-2, 7, and 9 are elevated in association with human immunodeficiency virus dementia. Ann. Neurol. 46, 391–398. [PubMed: 10482270]

Conant K, Wang Y, Szklarczyk A, Dudak A, Mattson MP, Lim ST, 2010. Matrix metalloproteinase-dependent shedding of intercellular adhesion molecule-5 occurs with long-term potentiation. Neuroscience 166, 508–521. [PubMed: 20045450]

Conant K, Allen M, Lim ST, 2015. Activity dependent CAM cleavage and neurotransmission. Front. Cell. Neurosci. 9, 305. [PubMed: 26321910]

Corder EH, Saunders AM, Strittmatter WJ, Schmechel DE, Gaskell PC, Small GW, Roses AD, Haines JL, Pericak-Vance MA, 1993. Gene dose of apolipoprotein E type 4 allele and the risk of Alzheimer's disease in late onset families. Science 261, 921–923. [PubMed: 8346443]

Crocker SJ, Milner R, Pham-Mitchell N, Campbell IL, 2006. Cell and agonist-specific regulation of genes for matrix metalloproteinases and their tissue inhibitors by primary glial cells. J. Neurochem. 98, 812–823. [PubMed: 16893421]

Deb S, Gottschall PE, 1996. Increased production of matrix metalloproteinases in enriched astrocyte and mixed hippocampal cultures treated with beta-amyloid peptides. J. Neurochem. 66, 1641–1647. [PubMed: 8627321]

DeWitt DA, Silver J, Canning DR, Perry G, 1993. Chondroitin sulfate proteoglycans are associated with the lesions of Alzheimer's disease. Exp. Neurol. 121, 149–152. [PubMed: 8339766]

Dubisova J, Burianova JS, Svobodova L, Makovicky P, Martinez-Varea N, Cimpean A, Fawcett JW, Kwok JCF, Kubinova S, 2022. Oral treatment of 4-methylumbelliferone reduced perineuronal nets and improved recognition memory in mice. Brain Res. Bull. 181, 144–156. [PubMed: 35066096]

Dumanis SB, Tesoriero JA, Babus LW, Nguyen MT, Trotter JH, Ladu MJ, Weeber EJ, Turner RS, Xu B, Rebeck GW, Hoe HS, 2009. ApoE4 decreases spine density and dendritic complexity in cortical neurons in vivo. J. Neurosci. 29, 15317–15322. [PubMed: 19955384]

Foscarin S, Raha-Chowdhury R, Fawcett JW, Kwok JCF, 2017. Brain ageing changes proteoglycan sulfation, rendering perineuronal nets more inhibitory. Aging (Albany NY) 9, 1607–1622. [PubMed: 28657900]

Fragkouli A, Tsilibary EC, Tzinia AK, 2014. Neuroprotective role of MMP-9 overexpression in the brain of Alzheimer's 5xFAD mice. Neurobiol. Dis. 70, 179–189. [PubMed: 25008761]

Ganguly K, Rejmak E, Mikosz M, Nikolaev E, Knapska E, Kaczmarek L, 2013. Matrix metalloproteinase (MMP) 9 transcription in mouse brain induced by fear learning. J. Biol. Chem. 288, 20978–20991. [PubMed: 23720741]

Gillespie AK, Jones EA, Lin YH, Karlsson MP, Kay K, Yoon SY, Tong LM, Nova P, Carr JS, Frank LM, Huang Y, 2016. Apolipoprotein E4 causes age-dependent disruption of slow gamma oscillations during hippocampal sharp-wave ripples. Neuron 90, 740–751. [PubMed: 27161522]

Halliday MR, Rege SV, Ma Q, Zhao Z, Miller CA, Winkler EA, Zlokovic BV, 2016. Accelerated pericyte degeneration and blood-brain barrier breakdown in apolipoprotein E4 carriers with Alzheimer's disease. J. Cereb. Blood Flow Metab. 36, 216–227. [PubMed: 25757756]

Hasel P, Rose IVL, Sadick JS, Kim RD, Liddelow SA, 2021. Neuroinflammatory astrocyte subtypes in the mouse brain. Nat. Neurosci. 24, 1475–1487. [PubMed: 34413515]

Hebisch M, Klostermeier S, Wolf K, Boccaccini AR, Wolf SE, Tanzi RE, Kim DY, 2023. The impact of the cellular environment and aging on modeling Alzheimer's disease in 3D cell culture models. Adv Sci (Weinh) e2205037. [PubMed: 36642841]

Ho MH, Yen CH, Hsieh TH, Kao TJ, Chiu JY, Chiang YH, Hoffer BJ, Chang WC, Chou SY, 2021. CCL5 via GPX1 activation protects hippocampal memory function after mild traumatic brain injury. Redox Biol. 46, 102067. [PubMed: 34315111]

Hoe HS, Cooper MJ, Burns MP, Lewis PA, van der Brug M, Chakraborty G, Cartagena CM, Pak DT, Cookson MR, Rebeck GW, 2007. The metalloprotease inhibitor TIMP-3 regulates amyloid precursor protein and apolipoprotein E receptor proteolysis. J. Neurosci. 27, 10895–10905. [PubMed: 17913923]

Hussler W, Hohn L, Stolz C, Vielhaber S, Garz C, Schmitt FC, Gundelfinger ED, Schreiber S, Seidenbecher CI, 2022. Brevican and Neurocan cleavage products in the cerebrospinal fluid - differential occurrence in ALS, epilepsy and Small vessel disease. Front. Cell. Neurosci. 16, 838432. [PubMed: 35480959]

Iaccarino HF, Singer AC, Martorell AJ, Rudenko A, Gao F, Gillingham TZ, Mathys H, Seo J, Kritskiy O, Abdurrob F, Adaikkan C, Canter RG, Rueda R, Brown EN, Boyden ES, Tsai LH, 2016. Gamma frequency entrainment attenuates amyloid load and modifies microglia. Nature 540, 230–235. [PubMed: 27929004]

Jones EA, Gillespie AK, Yoon SY, Frank LM, Huang Y, 2019. Early hippocampal sharp-wave ripple deficits predict later learning and memory impairments in an Alzheimer's disease mouse model. Cell Rep. 29 (2123–2133), e2124.

Joy MT, Ben Assayag E, Shabashov-Stone D, Liraz-Zaltsman S, Mazzitelli J, Arenas M, Abduljawad N, Kliper E, Korczyn AD, Thareja NS, Kesner EL, Zhou M, Huang S, Silva TK, Katz N, Bornstein NM, Silva AJ, Shohami E, Carmichael ST, 2019. CCR5 is a therapeutic target for recovery after stroke and traumatic brain injury. Cell 176 (1143–1157), e1113.

Kim J, Basak JM, Holtzman DM, 2009. The role of apolipoprotein E in Alzheimer's disease. Neuron 63, 287–303. [PubMed: 19679070]

Klein AS, Donoso JR, Kempter R, Schmitz D, Beed P, 2016. Early cortical changes in gamma oscillations in Alzheimer's disease. Front. Syst. Neurosci. 10, 83. [PubMed: 27833535]

Klemz A, Wildner F, Tutuncu E, Gerevich Z, 2021. Regulation of hippocampal gamma oscillations by modulation of intrinsic neuronal excitability. Front Neural Circuits 15, 778022. [PubMed: 35177966]

Knight BE, Kozlowski N, Havelin J, King T, Crocker SJ, Young EE, Baumbauer KM, 2019. TIMP-1 attenuates the development of inflammatory pain through MMP-dependent and receptor-mediated cell signaling mechanisms. Front. Mol. Neurosci. 12, 220. [PubMed: 31616247]

Korwek KM, Trotter JH, Ladu MJ, Sullivan PM, Weeber EJ, 2009. ApoE isoform-dependent changes in hippocampal synaptic function. Mol. Neurodegener. 4, 21. [PubMed: 19725929]

Lanfranco MF, Mocchetti I, Burns MP, Villapol S, 2017. Glial- and neuronal-specific expression of CCL5 mRNA in the rat brain. Front. Neuroanat. 11, 137. [PubMed: 29375328]

Lanfranco MF, Sepulveda J, Kopetsky G, Rebeck GW, 2021. Expression and secretion of apoE isoforms in astrocytes and microglia during inflammation. Glia 69, 1478–1493. [PubMed: 33556209]

Lee R, Kermani P, Teng KK, Hempstead BL, 2001. Regulation of cell survival by secreted proneurotrophins. Science 294, 1945–1948. [PubMed: 11729324]

Lensjo KK, Lepperod ME, Dick G, Hafting T, Fyhn M, 2017. Removal of Perineuronal nets unlocks juvenile plasticity through network mechanisms of decreased inhibition and increased gamma activity. J. Neurosci. 37, 1269–1283. [PubMed: 28039374]

Lepelletier FX, Mann DM, Robinson AC, Pinteaux E, Boutin H, 2017. Early changes in extracellular matrix in Alzheimer's disease. Neuropathol. Appl. Neurobiol. 43, 167–182. [PubMed: 26544797]

Logsdon AF, Francis KL, Richardson NE, Hu SJ, Faber CL, Phan BA, Nguyen V, Setthavongsack N, Banks WA, Woltjer RL, Keene CD, Latimer CS, Schwartz MW, Scarlett JM, Alonge KM, 2022. Decoding perineuronal net glycan sulfation patterns in the Alzheimer's disease brain. Alzheimers Dement. 18, 942–954. [PubMed: 34482642]

Lonskaya I, Partridge J, Lalchandani RR, Chung A, Lee T, Vicini S, Hoe HS, Lim ST, Conant K, 2013. Soluble ICAM-5, a product of activity dependent proteolysis, increases mEPSC frequency and dendritic expression of GluA1. PLoS One 8, e69136. [PubMed: 23844251]

Lorente L, Martin M, Plasencia F, Sole-Violan J, Blanquer J, Labarta L, Diaz C, Borreguero-Leon JM, Jimenez A, Paramo JA, Orbe J, Rodriguez JA, Salido E, 2013. The 372 T/C genetic polymorphism of TIMP-1 is associated with serum levels of TIMP-1 and survival in patients with severe sepsis. Crit. Care 17, R94. [PubMed: 23706069]

Martin-de-Saavedra MD, Santos MD, Penzes P, 2022. Intercellular signaling by ectodomain shedding at the synapse. Trends Neurosci. 45, 483–498. [PubMed: 35430102]

Meucci O, Fatatis A, Simen AA, Bushell TJ, Gray PW, Miller RJ, 1998. Chemokines regulate hippocampal neuronal signaling and gp120 neurotoxicity. Proc. Natl. Acad. Sci. U. S. A. 95, 14500–14505. [PubMed: 9826729]

Miyata S, Kitagawa H, 2017. Formation and remodeling of the brain extracellular matrix in neural plasticity: roles of chondroitin sulfate and hyaluronan. Biochim. Biophys. Acta Gen. Subj. 1861, 2420–2434. [PubMed: 28625420]

Montagne A, Nation DA, Sagare AP, Barisano G, Sweeney MD, Chakhoyan A, Pachicano M, Joe E, Nelson AR, D'Orazio LM, Buennagel DP, Harrington MG, Benzinger TLS, Fagan AM, Ringman JM, Schneider LS, Morris JC, Reiman EM, Caselli RJ, Chui HC, Tcw J, Chen Y, Pa J, Conti PS, Law M, Toga AW, Zlokovic BV, 2020. APOE4 leads to blood-brain barrier dysfunction predicting cognitive decline. Nature 581, 71–76. [PubMed: 32376954]

Mroczko B, Groblewska M, Zboch M, Kulczynska A, Koper OM, Szmitkowski M, Kornhuber J, Lewczuk P, 2014. Concentrations of matrix metalloproteinases and their tissue inhibitors in the cerebrospinal fluid of patients with Alzheimer's disease. J. Alzheimers Dis. 40, 351–357. [PubMed: 24448781]

Murase S, Lantz CL, Quinlan EM, 2017. Light reintroduction after dark exposure reactivates plasticity in adults via perisynaptic activation of MMP-9. Elife 6.

Murty DV, Manikandan K, Kumar WS, Ramesh RG, Purokayastha S, Nagendra B, Ml A, Balakrishnan A, Javali M, Rao NP, Ray S, 2021. Stimulus-induced gamma rhythms are weaker in human elderly with mild cognitive impairment and Alzheimer's disease. Elife 10.

Nagy V, Bozdagi O, Matynia A, Balcerzyk M, Okulski P, Dzwonek J, Costa RM, Silva AJ, Kaczmarek L, Huntley GW, 2006. Matrix metalloproteinase-9 is required for hippocampal late-phase long-term potentiation and memory. J. Neurosci. 26, 1923–1934. [PubMed: 16481424]

Nakamura H, Fujii Y, Inoki I, Sugimoto K, Tanzawa K, Matsuki H, Miura R, Yamaguchi Y, Okada Y, 2000. Brevican is degraded by matrix metalloproteinases and aggrecanase-1 (ADAMTS4) at different sites. J. Biol. Chem. 275, 38885–38890. [PubMed: 10986281]

Okulski P, Jay TM, Jaworski J, Duniec K, Dzwonek J, Konopacki FA, Wilczynski GM, Sanchez-Capelo A, Mallet J, Kaczmarek L, 2007. TIMP-1 abolishes MMP-9-dependent long-lasting long-term potentiation in the prefrontal cortex. Biol. Psychiatry 62, 359–362. [PubMed: 17210139]

Passman AM, Strauss RP, McSpadden SB, Finch-Edmondson M, Andrewartha N, Woo KH, Diepeveen LA, Zhao W, Fernandez-Irigoyen J, Santamaria E, Medina-Ruiz L, Szpakowska M, Chevigne A, Park H, Carlessi R, Tirnitz-Parker JEE, Blanco JR, London R, Callus BA, Elsegood CL, Baker MV, Martinez A, Yeoh GCT, Ochoa-Callejero L, 2021. Maraviroc prevents HCC development by suppressing macrophages and the liver progenitor cell response in a murine chronic liver disease model. Cancers (Basel) 13. [PubMed: 35008178]

Passos GF, Figueiredo CP, Prediger RD, Pandolfo P, Duarte FS, Medeiros R, Calixto JB, 2009. Role of the macrophage inflammatory protein-1alpha/CC chemokine receptor 5 signaling pathway in the neuroinflammatory response and cognitive deficits induced by beta-amyloid peptide. Am. J. Pathol. 175, 1586–1597. [PubMed: 19729478]

Peterson NB, Beeghly-Fadiel A, Gao YT, Long J, Cai Q, Shu XO, Zheng W, 2009. Polymorphisms in tissue inhibitors of metalloproteinases-2 and −3 and breast cancer susceptibility and survival. Int. J. Cancer 125, 844–850. [PubMed: 19431211]

Ping S, Qiu X, Kyle M, Zhao LR, 2021. Brain-derived CCR5 contributes to neuroprotection and brain repair after experimental stroke. Aging Dis. 12, 72–92. [PubMed: 33532129]

Plassman BL, Welsh-Bohmer KA, Bigler ED, Johnson SC, Anderson CV, Helms MJ, Saunders AM, Breitner JC, 1997. Apolipoprotein E epsilon 4 allele and hippocampal volume in twins with normal cognition. Neurology 48, 985–989. [PubMed: 9109888]

Poirier J, Davignon J, Bouthillier D, Kogan S, Bertrand P, Gauthier S, 1993. Apolipoprotein E polymorphism and Alzheimer's disease. Lancet 342, 697–699. [PubMed: 8103819]

Rebeck GW, Reiter JS, Strickland DK, Hyman BT, 1993. Apolipoprotein E in sporadic Alzheimer's disease: allelic variation and receptor interactions. Neuron 11, 575–580. [PubMed: 8398148]

Riddell DR, Zhou H, Atchison K, Warwick HK, Atkinson PJ, Jefferson J, Xu L, Aschmies S, Kirksey Y, Hu Y, Wagner E, Parratt A, Xu J, Li Z, Zaleska MM, Jacobsen JS, Pangalos MN, Reinhart PH, 2008. Impact of apolipoprotein E (ApoE) polymorphism on brain ApoE levels. J. Neurosci. 28, 11445–11453. [PubMed: 18987181]

Rivera S, 2019. Metalloproteinases in nervous system function and pathology: introduction. Cell. Mol. Life Sci. 76, 3051–3053. [PubMed: 31175371]

Sasaki Y, Kimura N, Aso Y, Yabuuchi K, Aikawa M, Matsubara E, 2021. Relationship between cerebrospinal fluid matrix metalloproteinases levels and brain amyloid deposition in mild cognitive impairment. Biomolecules 11. [PubMed: 35053159]

Scarlett JM, Hu SJ, Alonge KM, 2022. The "loss" of Perineuronal nets in Alzheimer's disease: missing or hiding in plain sight? Front. Integr. Neurosci. 16, 896400. [PubMed: 35694184]

Seidenbecher CI, Richter K, Rauch U, Fassler R, Garner CC, Gundelfinger ED, 1995. Brevican, a chondroitin sulfate proteoglycan of rat brain, occurs as secreted and cell surface glycosylphosphatidylinositol-anchored isoforms. J. Biol. Chem. 270, 27206–27212. [PubMed: 7592978]

Shaw P, Lerch JP, Pruessner JC, Taylor KN, Rose AB, Greenstein D, Clasen L, Evans A, Rapoport JL, Giedd JN, 2007. Cortical morphology in children and adolescents with different apolipoprotein E gene polymorphisms: an observational study. Lancet Neurol. 6, 494–500. [PubMed: 17509484]

Shen Y, Zhou M, Cai D, Filho DA, Fernandes G, Cai Y, de Sousa AF, Tian M, Kim N, Lee J, Necula D, Zhou C, Li S, Salinas S, Liu A, Kang X, Kamata M, Lavi A, Huang S, Silva T, Do Heo W, Silva AJ, 2022. CCR5 closes the temporal window for memory linking. Nature 606, 146–152. [PubMed: 35614219]

Shoji H, Hagihara H, Takao K, Hattori S, Miyakawa T, 2012. T-maze forced alternation and left-right discrimination tasks for assessing working and reference memory in mice. J. Vis. Exp. (60), 3300. [PubMed: 22395674]

Small GW, Mazziotta JC, Collins MT, Baxter LR, Phelps ME, Mandelkern MA, Kaplan A, La Rue A, Adamson CF, Chang L, et al. , 1995. Apolipoprotein E type 4 allele and cerebral glucose metabolism in relatives at risk for familial Alzheimer disease. JAMA 273, 942–947. [PubMed: 7884953]

Smith AC, Kupchik YM, Scofield MD, Gipson CD, Wiggins A, Thomas CA, Kalivas PW, 2014. Synaptic plasticity mediating cocaine relapse requires matrix metalloproteinases. Nat. Neurosci. 17, 1655–1657. [PubMed: 25326689]

Strittmatter WJ, Saunders AM, Schmechel D, Pericak-Vance M, Enghild J, Salvesen GS, Roses AD, 1993. Apolipoprotein E: high-avidity binding to beta-amyloid and increased frequency of type 4 allele in late-onset familial Alzheimer disease. Proc. Natl. Acad. Sci. U. S. A. 90, 1977–1981. [PubMed: 8446617]

Sullivan PM, Mezdour H, Aratani Y, Knouff C, Najib J, Reddick RL, Quarfordt SH, Maeda N, 1997. Targeted replacement of the mouse apolipoprotein E gene with the common human APOE3 allele enhances diet-induced hypercholesterolemia and atherosclerosis. J. Biol. Chem. 272, 17972–17980. [PubMed: 9218423]

Sun ZY, Bozzelli PL, Caccavano A, Allen M, Balmuth J, Vicini S, Wu JY, Conant K, 2018. Disruption of perineuronal nets increases the frequency of sharp wave ripple events. Hippocampus 28, 42–52. [PubMed: 28921856]

Szklarczyk A, Lapinska J, Rylski M, McKay RD, Kaczmarek L, 2002. Matrix metalloproteinase-9 undergoes expression and activation during dendritic remodeling in adult hippocampus. J. Neurosci. 22, 920–930. [PubMed: 11826121]

Tai LM, Ghura S, Koster KP, Liakaite V, Maienschein-Cline M, Kanabar P, Collins N, Ben-Aissa M, Lei AZ, Bahroos N, Green SJ, Hendrickson B, Van Eldik LJ, LaDu MJ, 2015. APOE-modulated Abeta-induced neuroinflammation in Alzheimer's disease: current landscape, novel data, and future perspective. J. Neurochem. 133, 465–488. [PubMed: 25689586]

Tcw J, Qian L, Pipalia NH, Chao MJ, Liang SA, Shi Y, Jain BR, Bertelsen SE, Kapoor M, Marcora E, Sikora E, Andrews EJ, Martini AC, Karch CM, Head E, Holtzman DM, Zhang B, Wang M, Maxfield FR, Poon WW, Goate AM, 2022. Cholesterol and matrisome pathways dysregulated in astrocytes and microglia. Cell 185 (2213–2233), e2225.

Tian L, Stefanidakis M, Ning L, Van Lint P, Nyman-Huttunen H, Libert C, Itohara S, Mishina M, Rauvala H, Gahmberg CG, 2007. Activation of NMDA receptors promotes dendritic spine development through MMP-mediated ICAM-5 cleavage. J. Cell Biol. 178, 687–700. [PubMed: 17682049]

Traikapi A, Konstantinou N, 2021. Gamma oscillations in Alzheimer's disease and their potential therapeutic role. Front. Syst. Neurosci. 15, 782399. [PubMed: 34966263]

Trommer BL, Shah C, Yun SH, Gamkrelidze G, Pasternak ES, Ye GL, Sotak M, Sullivan PM, Pasternak JF, LaDu MJ, 2004. ApoE isoform affects LTP in human targeted replacement mice. Neuroreport 15, 2655–2658. [PubMed: 15570172]

Trommer BL, Shah C, Yun SH, Gamkrelidze G, Pasternak ES, Stine WB, Manelli A, Sullivan P, Pasternak JF, LaDu MJ, 2005. ApoE isoform-specific effects on LTP: blockade by oligomeric amyloid-beta1–42. Neurobiol. Dis. 18, 75–82. [PubMed: 15649697]

Turner RS, Thomas RG, Craft S, van Dyck CH, Mintzer J, Reynolds BA, Brewer JB, Rissman RA, Raman R, Aisen PS, Alzheimer's Disease Cooperative S, 2015. A randomized, double-blind, placebo-controlled trial of resveratrol for Alzheimer disease. Neurology 85, 1383–1391. [PubMed: 26362286]

Venturino A, Schulz R, De Jesus-Cortes H, Maes ME, Nagy B, Reilly-Andujar F, Colombo G, Cubero RJA, Schoot Uiterkamp FE, Bear MF, Siegert S, 2021. Microglia enable mature perineuronal nets disassembly upon anesthetic ketamine exposure or 60-Hz light entrainment in the healthy brain. Cell Rep. 36, 109313. [PubMed: 34233180]

Wang C, Wilson WA, Moore SD, Mace BE, Maeda N, Schmechel DE, Sullivan PM, 2005. Human apoE4-targeted replacement mice display synaptic deficits in the absence of neuropathology. Neurobiol. Dis. 18, 390–398. [PubMed: 15686968]

Wang XB, Bozdagi O, Nikitczuk JS, Zhai ZW, Zhou Q, Huntley GW, 2008. Extracellular proteolysis by matrix metalloproteinase-9 drives dendritic spine enlargement and long-term potentiation coordinately. Proc. Natl. Acad. Sci. U. S. A. 105, 19520–19525. [PubMed: 19047646]

Weekman EM, Wilcock DM, 2016. Matrix metalloproteinase in blood-brain barrier breakdown in dementia. J. Alzheimers Dis. 49, 893–903. [PubMed: 26599057]

Welser-Alves JV, Crocker SJ, Milner R, 2011. A dual role for microglia in promoting tissue inhibitor of metalloproteinase (TIMP) expression in glial cells in response to neuroinflammatory stimuli. J. Neuroinflammation 8, 61. [PubMed: 21631912]

Wiera G, Nowak D, van Hove I, Dziegiel P, Moons L, Mozrzymas JW, 2017. Mechanisms of NMDA receptor- and voltage-gated L-type Calcium Channel-dependent hippocampal LTP critically rely on proteolysis that is mediated by distinct metalloproteinases. J. Neurosci. 37, 1240–1256. [PubMed: 28069922]

Wojtowicz T, Mozrzymas JW, 2014. Matrix metalloprotease activity shapes the magnitude of EPSPs and spike plasticity within the hippocampal CA3 network. Hippocampus 24, 135–153. [PubMed: 24115249]

Xu PT, Schmechel D, Rothrock-Christian T, Burkhart DS, Qiu HL, Popko B, Sullivan P, Maeda N, Saunders AM, Roses AD, Gilbert JR, 1996. Human apolipoprotein E2, E3, and E4 isoform-specific transgenic mice: human-like pattern of glial and neuronal immunoreactivity in central nervous system not observed in wild-type mice. Neurobiol. Dis. 3, 229–245. [PubMed: 8980023]

Yan P, Hu X, Song H, Yin K, Bateman RJ, Cirrito JR, Xiao Q, Hsu FF, Turk JW, Xu J, Hsu CY, Holtzman DM, Lee JM, 2006. Matrix metalloproteinase-9 degrades amyloid-beta fibrils in vitro and compact plaques in situ. J. Biol. Chem. 281, 24566–24574. [PubMed: 16787929]

Yang S, Cacquevel M, Saksida LM, Bussey TJ, Schneider BL, Aebischer P, Melani R, Pizzorusso T, Fawcett JW, Spillantini MG, 2015. Perineuronal net digestion with chondroitinase restores memory in mice with tau pathology. Exp. Neurol. 265, 48–58. [PubMed: 25483398]

Yin KJ, Cirrito JR, Yan P, Hu X, Xiao Q, Pan X, Bateman R, Song H, Hsu FF, Turk J, Xu J, Hsu CY, Mills JC, Holtzman DM, Lee JM, 2006. Matrix metalloproteinases expressed by astrocytes mediate extracellular amyloid-beta peptide catabolism. J. Neurosci. 26, 10939–10948. [PubMed: 17065436]

Yin C, Ackermann S, Ma Z, Mohanta SK, Zhang C, Li Y, Nietzsche S, Westermann M, Peng L, Hu D, Bontha SV, Srikakulapu P, Beer M, Megens RTA, Steffens S, Hildner M, Halder LD, Eckstein HH, Pelisek J, Herms J, Roeber S, Arzberger T, Borodovsky A, Habenicht L, Binder CJ, Weber C, Zipfel PF, Skerka C, Habenicht AJR, 2019. ApoE attenuates unresolvable inflammation by complex formation with activated C1q. Nat. Med. 25, 496–506. [PubMed: 30692699]

Zhou M, Greenhill S, Huang S, Silva TK, Sano Y, Wu S, Cai Y, Nagaoka Y, Sehgal M, Cai DJ, Lee YS, Fox K, Silva AJ, 2016. CCR5 is a suppressor for cortical plasticity and hippocampal learning and memory. Elife 5.

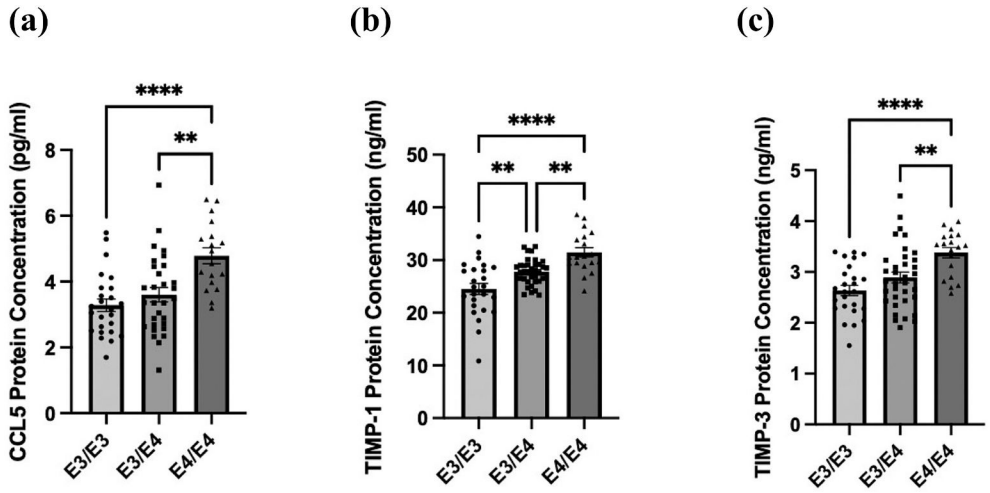

Fig. 1.

APOE4/E4 AD patients have significantly higher CCL5 protein concentrations detected in CSF as compared to *APOE3/E3* and *APOE3/E4* AD patients ($p < 0.0001$ and $p = 0.0012$, respectively, ANOVA with Tukey's *post hoc* multiple comparisons), as measured by ELISA (a). *APOE4/E4* AD patients also have elevated levels of TIMP-3 protein concentrations as compared to *APOE3/E3* and *APOE3/E4* AD patients (c; $p < 0.0001$ and $p = 0.0068$ respectively, ANOVA with Tukey's *post hoc* multiple comparisons), as detected by ELISA. Both *APOE3/E4* and *APOE4/E4* AD patients have significantly higher TIMP-1 protein concentration (b), as compared to *APOE3/E3* patients ($p = 0.0049$ and $p = 0.0033$, respectively, ANOVA with Tukey's *post hoc* multiple comparison, $n \geq 18$ CSF samples per genotype for all analytes).

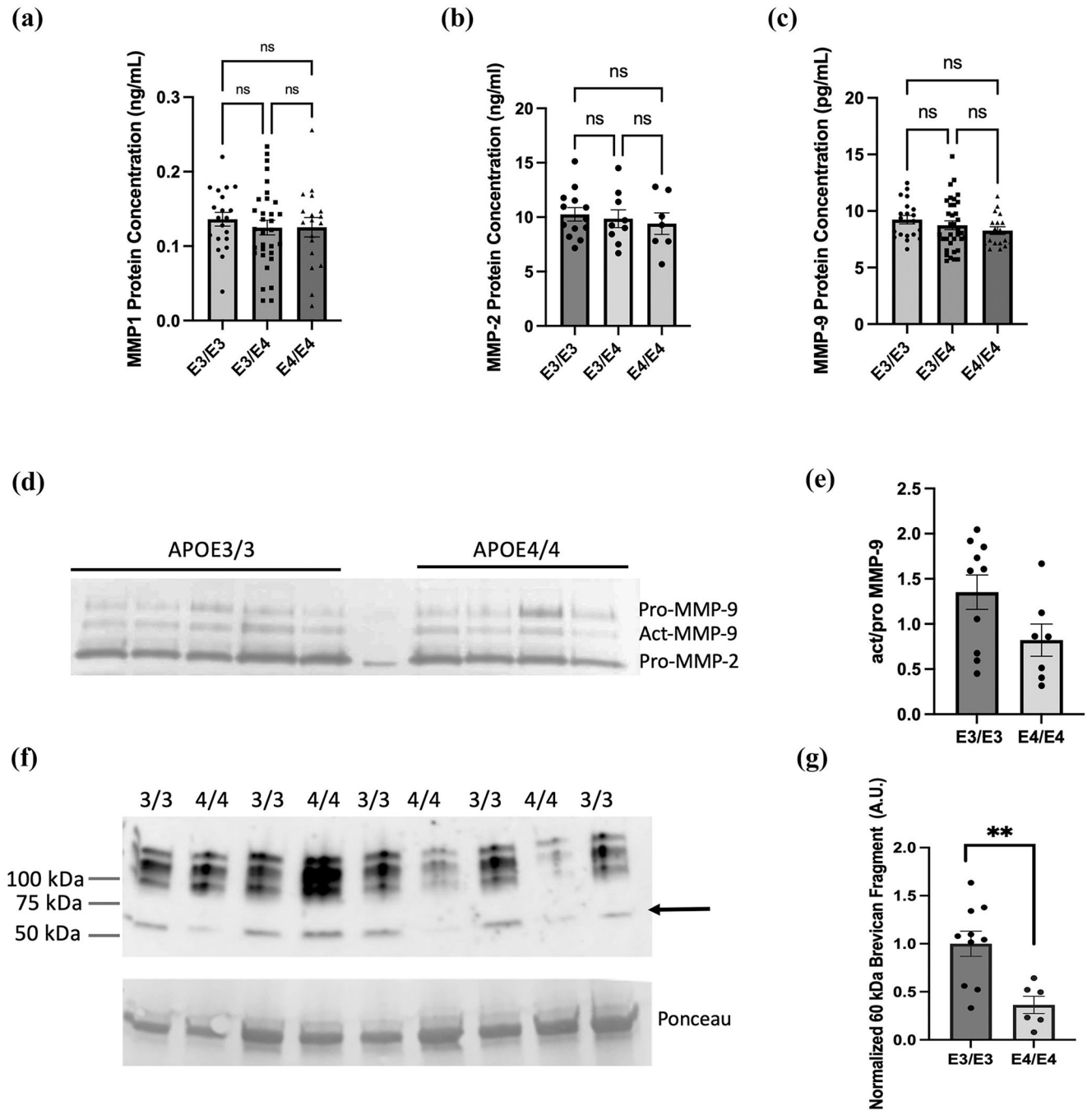

Fig. 2.

MMP-1, MMP-2, and MMP-9 protein levels (a-c) do not show differences as a function of AD patient *APOE* genotype. Note: fewer samples were analyzed for MMP-2 because many pre-treatment samples had been depleted and thus 52-week post-placebo samples were instead used for this assay as described in the methods section. Representative gelatin substrate zymography (d) and Western blot images on 10 post-placebo *APOE3/E3* CSF samples and 7 post-placebo *APOE4/E4* samples are also shown (f). The ratio of active to pro MMP-9 was non-significantly reduced in *APOE4/E4* samples (d, e; $p = 0.07$) but levels of a

50–60 kDa metalloproteinase brevican cleavage fragment (arrow) was significantly reduced in *APOE4/E4* samples (f, g; $p = 0.0039$, Student's *t*-test). Note, one outlier was removed.

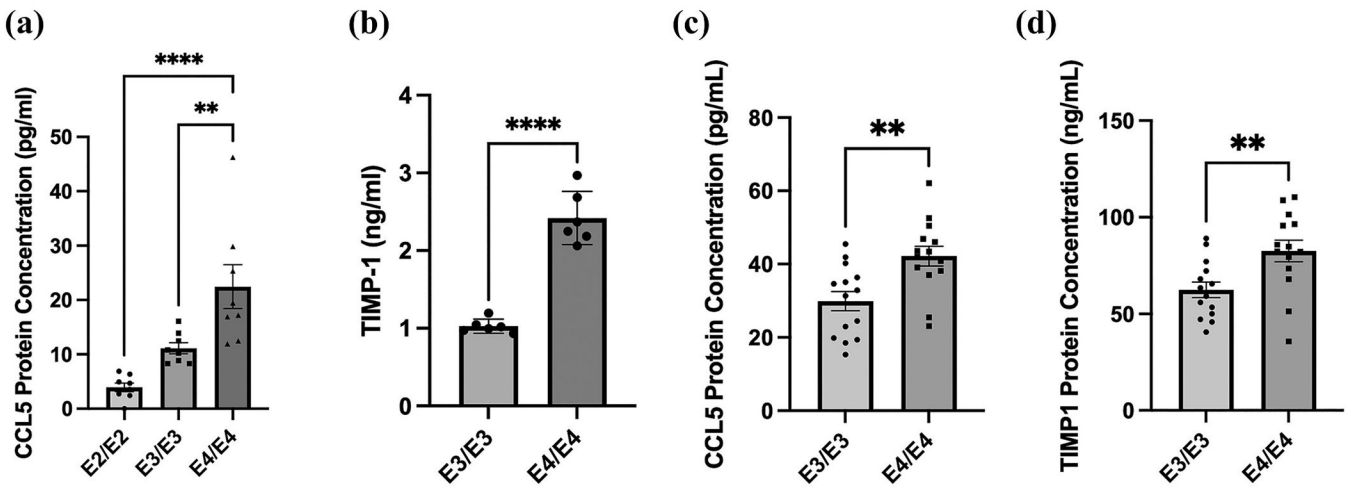

Fig. 3.

CCL5 and TIMP-1 are increased in astrocyte supernatants and brain lysates from *APOE4* TR mice. (a, b) Supernatants from *APOE3/E3* TR and *APOE4/E4* TR astrocytes were collected and analyzed *via* ELISA. As shown in 3a and 3b respectively, CCL5 and TIMP-1 levels are increased in *APOE4/E4* TR murine astrocyte supernatants. CCL5 levels in *APOE4/E4* are significantly increased as compared to *APOE3/E3* or *APOE2/E2* ($p = 0.0001$ and $p < 0.0095$, ANOVA with Tukey's *post hoc* multiple comparisons) and TIMP-1 levels were increased in *APOE4/E4* as compared to *APOE3/E3* ($p < 0.0001$, Student's *t*-test). ELISA results for hippocampal lysates from *APOE3/E3* and *APOE4/E4* TR mice are shown in Figs. 3c–d and demonstrate that both CCL5 and TIMP-1 are increased in *APOE4/E4* TR lysates ($n = 14$, $p = 0.0029$ and 0.0069 respectively, Students t-test).

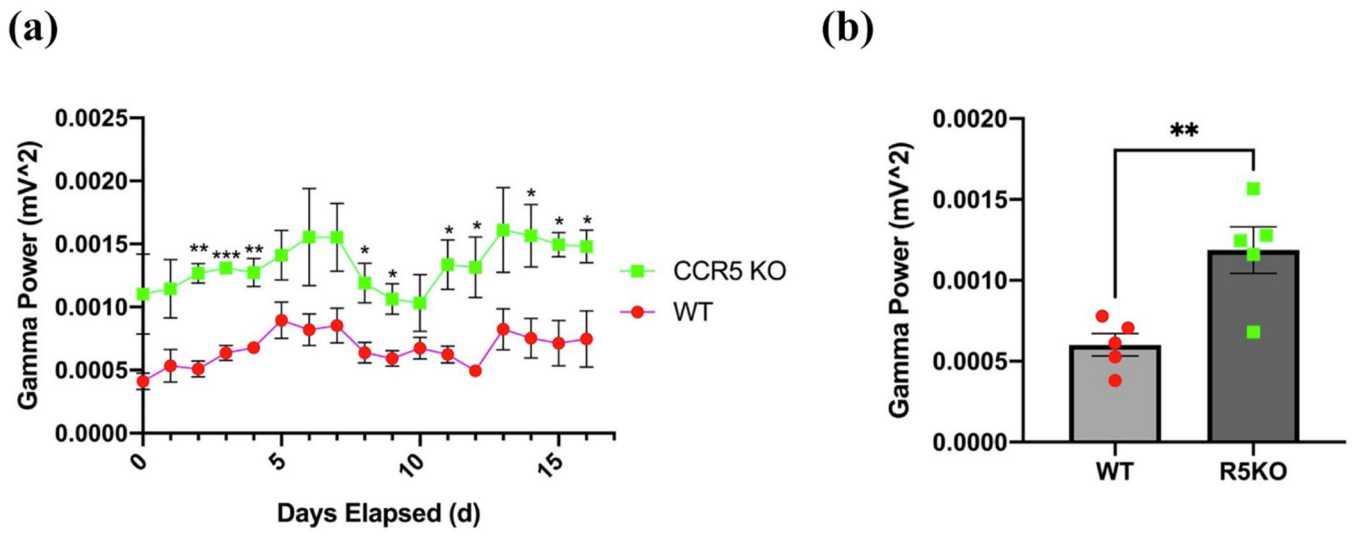

Fig. 4.

Gamma power (20 – 55 Hz) is significantly increased in *CCR5*KO mice compared to age-matched wild-type mice (4a; $p = 0.0063$; $n = 5$ per genotype). EEG activity was recorded over a 2-week period, and gamma power was calculated for a 60-min interval once every two hours during the dark/active phase (6 pm- 6 am; average of power from $n = 6$ one-hour recording epochs). Days elapsed indicates EEG data recorded after animals had fully recovered from the implantation surgery. The average value for each animal over all days is shown in 4b.

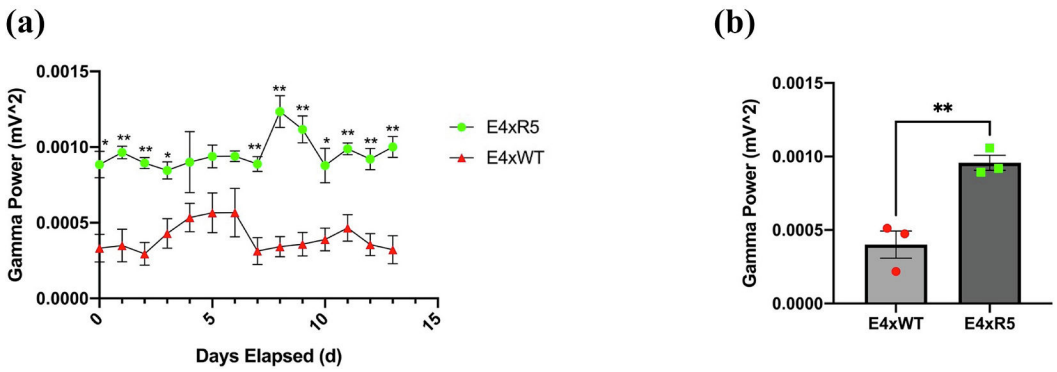

Fig. 5.

Gamma power (20 – 55 Hz) is significantly increased in *APOE4 TR*/*CCR5*KO heterozygous mice as compared to age-matched *APOE4 TR*/wild-type mice (right panel; $p = 0.0062$; $n = 3$ per genotype). Gamma power was again calculated for a 60-min interval once every two hours during the dark/active phase (6 pm- 6 am; average of power from n = 6 one-hour recording epochs) as shown in 5a. Days elapsed indicates EEG data recorded after animals had fully recovered from the implantation surgery. The average value for each animal over all days is shown in 5b.

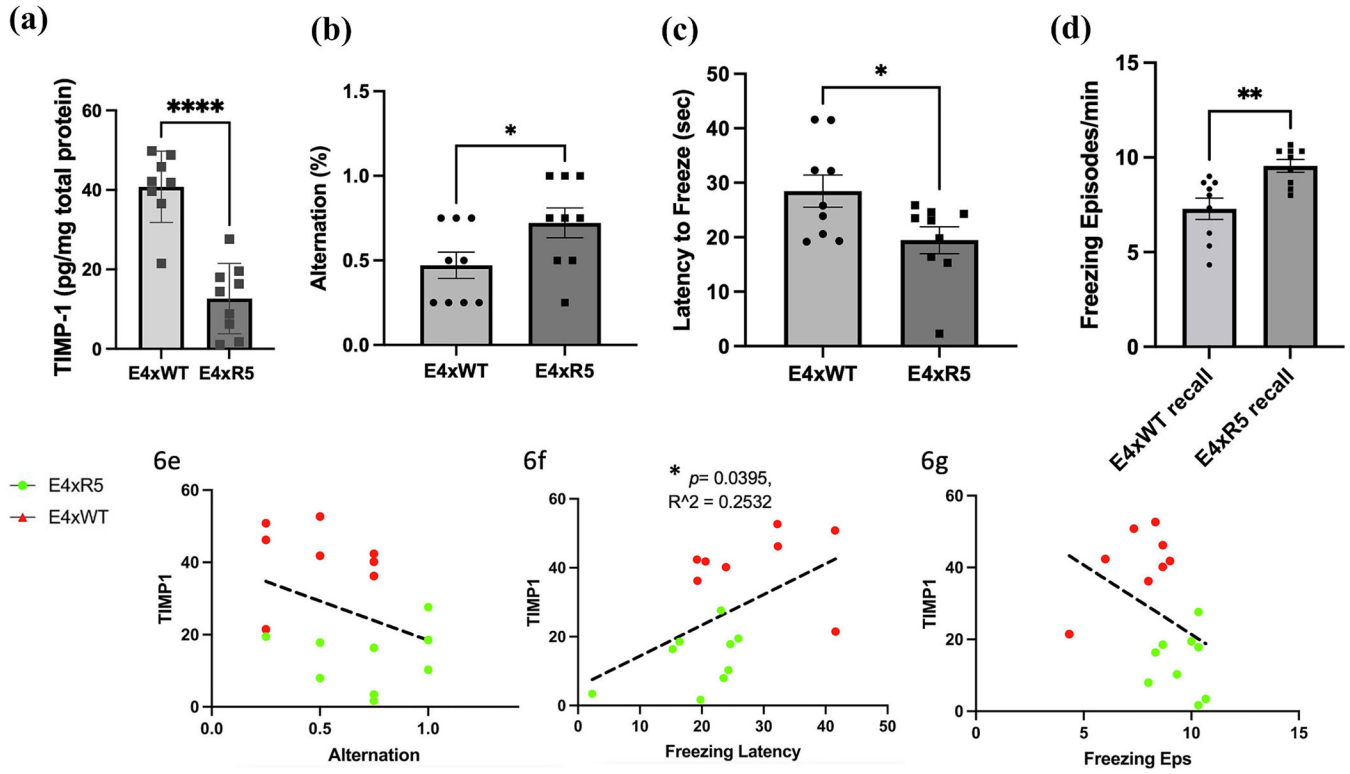

Fig. 6.

APOE4 TR/*CCR5*KO heterozygous mice have reduced hippocampal TIMP-1 levels as well as improved working and long-term memory. Hippocampal lysates from *APOE4 TR*/*CCR5*KO and *APOE4* TR/wild-type heterozygotes were collected and analyzed *via* ELISA for TIMP-1. TIMP-1 levels are substantially reduced in the CCR5 heterozygous knockout lysates (a; $p = 0.0001$, Student's *t*-test, $n = 8–9$ per group). (b-d) Before sacrificing the mice, working and long-term memory were assessed using the T-maze and fear conditioning tasks. *APOE4 TR*/*CCR5*KO heterozygous mice have significantly increased alternation rate between the arms of the T-maze as compared to age-matched *APOE4 TR*/ wild-type heterozygous mice (b: $p = 0.0485$). *APOE4 TR*/*CCR5*KO heterozygous mice had significantly more freezing episodes per minute in the recall trial of the fear conditioning task (d; $p = 0.0032$), and a significantly reduced latency to freeze on the trial day (c: $p = 0.0328$). Correlation analyses for TIMP-1 and behavioral endpoints are shown in 6 e-g. A correlation between higher TIMP-1 levels and longer latency to freeze was observed (6f: $p = 0.0396$). No differences were observed in freezing episodes per minute during training (not shown).

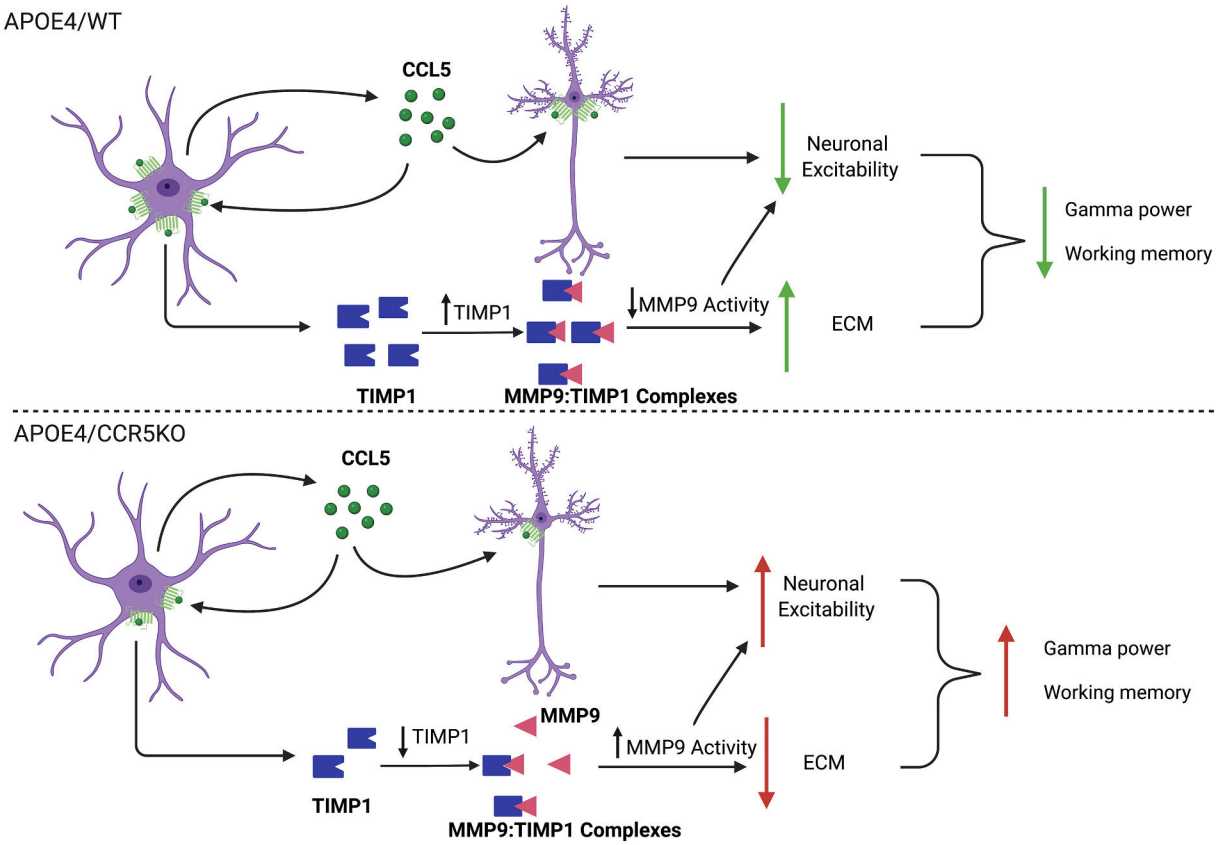

Fig. 7.

Hypothetical mechanisms by which APOE4 and CCL5 could reduce excitatory neurotransmission. As shown in the upper panel, *APOE4* TR astrocytes express increased CCL5 which engages G protein coupled receptors on astrocytes and neurons. CCL5/CCR5 signaling in pyramidal neurons reduces their excitability (Shen et al., 2022), while CCL5/CCR5 signaling in astrocytes could increase TIMP-1 levels to reduce MMP-9 dependent LTP and ECM attenuation. As shown in the lower panel, knockdown of CCR5 will reduce CCL5-mediated pyramidal cell inhibition. CCR5 knockdown may also reduce astrocytic expression of TIMP-1 and thus allow MMP-9 to facilitate pyramidal excitability ECM attenuation. This figure was created with http://Biorender.com

Table 1

Baseline CSF sample patient demographics.

Genotype	Age (average ± SEM)	Male/Female (n, %)
APOE3/3	72.24 ± 1.476	14, 42.4% / 19, 57.6%
APOE3/4	73.65 ± 1.043	22, 43.1% / 29, 56.9%
APOE4/4	69.87 ± 2.223	9, 39.1% / 14, 60.9%

Table 2

52-week post-placebo CSF sample patient demographics.

Genotype	Age (average ± SEM)	Male/Female (n, %)
APOE3/3	75.5 ± 2.4	5, 38.46% / 8, 61.53%
APOE3/4	75.4 ± 1.97	5, 55.56% / 4, 44.44%
APOE4/4	70.85 ± 6.04	4, 57.14% / 3, 42.86%